Journal of Industrial and Engineering Chemistry xxx (2017) xxx–xxx

Contents lists available at ScienceDirect

Journal of Industrial and Engineering Chemistry

journal homepage: www.elsevier.com/locate/jiec

Band structure of amorphous zinc tin oxide thin films deposited by atomic layer deposition

Sunyoung Lee[1], Sungjoon Kim[1], Seokhee Shin, Zhenyu Jin, Yo-Sep Min*

Department of Chemical Engineering, Konkuk University, 120 Neungdong-Ro, Gwangjin-Gu, Seoul 05029, Republic of Korea

ARTICLE INFO

Article history:
Received 17 August 2017
Received in revised form 23 September 2017
Accepted 24 September 2017
Available online xxx

Keywords:
Zinc tin oxide
Band structure
Atomic layer deposition
Work function
Buffer layer

ABSTRACT

Recently, zinc tin oxide (ZTO) has attracted attention as an alternative buffer layer to replace CdS for photovoltaic cells. ZTO thin films were grown by atomic layer deposition from diethylzinc, tetrakis (dimethylamido)tin, and water. Compositional, structural and optical properties were characterized to construct band diagram of the ZTO films depending on Sn content. The ZTO films exhibit optical bandgaps of 2.95–3.07 eV which are wider than that of CdS. Furthermore, their work function is also observed to vary in a wide range of 4.32–5.16 eV. It is attributed to incorporation of Sn into ZTO which strongly influences formation of oxygen vacancies.

Introduction

Thin-film photovoltaic (PV) cells directly and efficiently convert solar energy into electrical energy with the highest conversion efficiency of 22.6%, which has been observed for $Cu(In,Ga)Se_2$ (CIGS) solar cells [1]. Generally, thin-film PV cells such as CIGS solar cells require a buffer layer in their window layer stack to prevent unfavorable conduction band alignment that promotes interface recombination.

Commonly, *n*-type CdS is used as a buffer layer to sufficiently line up the conduction bands of chalcopyrite-type absorbers (e.g., CIGS, $CuGaSe_2$, $CuInSe_2$, or $Cu(In,Ga)(S,Se)_2$) and transparent ZnO in order to achieve high efficiency [2–4]. However, the disadvantages of using CdS as a buffer layer significantly overweigh its advantages. The CdS is usually prepared by non-vacuum chemical bath deposition, whereas CIGS absorbers are commonly grown under vacuum (e.g., by co-evaporation), and are air-sensitive. In addition to these differences, PV cells containing CdS buffer layers cannot be easily commercialized and produced on an industrial scale due to the toxicity of CdS and its relatively small bandgap (E_g = 2.42–2.45 eV), which results in absorption of the blue part in the solar spectrum by the CdS layer, not by the absorber layer. Hence, other buffer layer materials need to be developed to reduce the above optical loss and promote the industrial production of PV cells.

The extensive search for suitable buffer layer materials revealed that in thin-film solar cells, In_2S_3 and certain Cd-free Zn-based compounds (e.g., $ZnO_{1-x}S_x$, $Zn_{1-x}Mg_xO_y$, and $Zn_{1-x}Sn_xO_y$) prepared by atomic layer deposition (ALD) achieve high efficiencies comparable to that of CdS [4–8]. Notably, $Zn_{1-x}Sn_xO_y$ (ZTO) thin films grown by ALD showed high performance in CIGS cells, achieving conversion efficiencies of up to 18.0% [7].

The alignment of conduction band levels in the heterojunctions of a PV cell plays a significant role in reducing unnecessary recombination at junction interfaces. Recently, Kapilashrami et al. reported that hybridization between the oxygen and metal states of ZTO films gives rise to variation of conduction and valence band edges depending on the Sn content [9]. However, the work function of ZTO buffer layers has not been characterized in detail. Despite the conduction band offset being considered, the Fermi level of a buffer layer needs to be closely investigated, since an undesired barrier can be additionally created by band bending induced from Fermi level alignment at equilibrium. Meanwhile, in amorphous oxide semiconductors, oxygen vacancy formation is known to be closely related to the charge carrier generation [10]. Therefore, it is required to understand the correlation between oxygen vacancy and Fermi level of which position is varied by the carrier concentrations.

Here, we investigated compositional and structural characteristics of the ternary ZTO thin films grown by ALD by X-ray photoelectron spectroscopy (XPS) and X-ray diffraction (XRD). Their optical bandgaps and work functions were also studied to

* Corresponding author.
E-mail address: ysmin@konkuk.ac.kr (Y.-S. Min).
[1] These authors equally contributed to this work.

https://doi.org/10.1016/j.jiec.2017.09.045
1226-086X/

construct the band structures of the ZTO films, depending on the Sn content, by using UV-visible spectroscopy and Kelvin probe force microscopy (KPFM). In addition, by using the proposed band structure of the ZTO films, diode characteristics of *n*-ZnO/*p*-Si, *n*-SnO_2/*p*-Si and *n*-ZTO/*p*-Si heterojunction were interpreted for various Sn content.

Experimental

ZTO thin films were grown on boron-doped *p*-type Si (100) wafers with a resistivity of 10.0 Ω cm (LG Siltron, Inc.) at 150 °C in a laminar flow-type reactor (CN1 Co., Ltd.). Prior to the ALD process, the Si wafers were etched in dilute HF solution (1.63%) to clean and remove native SiO_2. For specimens to obtain optical bandgaps, the ZTO thin films were grown on polished quartz substrates (Hanjin Quartz). Tetrakis(dimethylamido)tin(IV) (TDMASn) and diethylzinc (DEZ) were used as Sn and Zn precursors (Nuri Tech Co.), and water was utilized as an oxygen precursor. Both DEZ (vapor pressure ~9.2 Torr at 15 °C [11]) and water were vaporized from external canisters into the reaction chamber at room temperature. However, due to the low vapor pressure (~0.04 Torr at 40 °C) of TDMASn [12], the canister of Sn precursor was heated to 50 °C, and N_2 (50 sccm, 99.999%) was used as a carrier gas. DEZ, TDMASn, and water vapors were introduced at feed rates of 1.3×10^{-4}, 3.2×10^{-5}, and 1.3×10^{-3} mol/s, respectively. Every precursor pulse was followed by N_2 purging at a flow rate of 400 sccm. All delivery lines were constantly maintained at 100 °C. The base pressure of the reaction chamber was less than 40 mTorr, and ALD was operated at a working pressure range of 300–600 mTorr.

Similarly to the ternary ALD processes described by Hultqvist et al. [6] and Mullings et al. [13], one ZTO supercycle consisted of several subcycles of ZnO and SnO_2 deposition. A typical ZnO deposition process was described by a sequence of DEZ-N_2-H_2O-N_2 pulses with lengths of 1-10-1-10 s. For optimizing the saturation time of the Sn precursor, SnO_2 deposition was performed using a sequence of TDMASn-N_2-H_2O-N_2 pulses with lengths of 1-10-2-30 s. The desired Sn and Zn contents of ZTO thin films were obtained by varying the corresponding fractions of ZnO and SnO_2 subcycles in the total number of subcycles. For example, in order to achieve the ALD-preset subcycle fraction [Sn/(Sn + Zn)] of ~0.4, one supercycle comprised three ZnO and two SnO_2 subcycles [2/(2 + 3) = 0.4].

The thickness of ZTO thin films was determined by spectroscopic ellipsometry (SE; MG-1000, NanoView Co., Ltd.). The incidence angle of polarized light in the SE was fixed at ~70°, and the energy of the incident light is ranged in 1.5–5.0 eV. XPS (PHI 5000 VersaProbe, Ulvac-PHI) utilizing monochromatic Al K_α emission was employed to characterize the elemental composition and chemical states of ZTO films, in which the C 1 s peak (284.8 eV) of the adventitious carbon was used as an internal reference for calibration. For cleaning the surface of specimens, Argon sputtering was performed for 10 s in the XPS chamber by bombarding Ar^+ ions (2 keV). X-ray diffraction (XRD; Philips X'pert Pro MRD) patterns were recorded at an incidence angle of 1.0° using Cu K_α emission. UV-visible spectroscopy (Mega900, scinco) was also performed to determine optical bandgaps of each film grown on quartz substrates. Surface potential measurements and topography were performed by kelvin prove force microscopy (KPFM; XE-100, Park systems) using a Au–Cr coated cantilever (NSC14–cr–au; tip height = 12–18 μm, tip radius ~35 nm, and resonant frequency of 142 Hz).

The electrical properties of ZTO thin films were characterized utilizing *n*-ZTO/*p*-Si heterojunction diodes with different Sn contents, in which the thickness of ZTO on Si was ~20 nm. Ohmic contacts were formed by thermal evaporation–deposition of Al and Au as top and bottom electrodes, respectively. The Al top electrode was deposited with a shadow mask with a circle area of $\sim 1.26 \times 10^{-3}$ cm^2. Current density–voltage (*J*–*V*) curves of the diodes were recorded using a semiconductor parameter analyzer (HP 4145B).

Results and discussion

Growth rate and structural characteristics

Fig. 1 shows the thicknesses of the grown films for a total of 100 subcycles (i.e., 20 supercycles and 5 subcycles in each supercycle) as a function of the ALD-preset subcycle fraction of Sn/(Sn + Zn). The growth rates of ZnO [Sn/(Sn + Zn) = 0] and SnO_2 [Sn/(Sn + Zn) = 1] at 150 °C are 1.80 and 0.82 Å/cycle, respectively, which are well consistent with those reported by Mullings et al. [13]. However, ZTO thin films are grown far slower than expected from the growth rates of ZnO and SnO_2 considering the ALD-preset subcycle fraction (for the nominally-predicted thickness, see the dashed line). The retardation of ZTO growth can be explained by slow nucleation [14] and the incomplete removal of precursor-bound ligands [15].

Fig. 2 shows the XRD patterns of ALD-grown thin films. The ZnO film exhibits three distinct peaks attributed to (100), (002), and (101) planes, which reveal a hexagonal wurtzite-type polycrystalline structure. In contrast, the SnO_2 and ZTO thin films are amorphous, not showing any noticeable peaks.

Topographical images (Fig. S1) also show that ZnO thin film has a higher root-mean-squared (rms) surface roughness (0.82 nm) than those (0.35–0.50 nm) of SnO_2 and ZTO thin films, owing to the amorphous nature, except for the ZTO film with 52% Sn content. Even though the film of 52% Sn is also amorphous in XRD, it shows much higher roughness (2.98 nm) indicating the presence of plateau-like surface structure with a size of ~300 nm. It may be attributed to atomic migration for phase separation of ZTO due to thermodynamic instability. Recently, Heo et al. also observed the phase separation in ALD-ZTO films, and their particle size was around 300 nm. The phase separation occurs at an annealing temperature lower than the crystallization temperature [16]. It indicates that one phase of the ZTO film with comparable amounts of Zn and Sn is thermodynamically less stable than the separated phases (Zn-rich and Sn-rich phases). Indeed, the depth profile (Fig. S2) of the film reveals that the Sn content severely decreases in the direction of depth, but the Zn content increases in the same

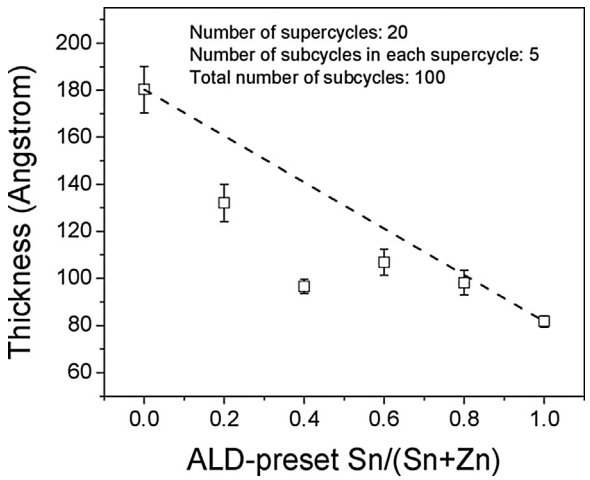

Fig. 1. Thickness of ZTO films as a function of the ALD-preset Sn/(Sn + Zn) subcycle fractions for a total of 100 subcycles at 150 °C. The dashed line indicates ZTO thickness expected from the growth rates of ZnO and SnO_2 growth.

Please cite this article in press as: S. Lee, et al., Band structure of amorphous zinc tin oxide thin films deposited by atomic layer deposition, J. Ind. Eng. Chem. (2017), https://doi.org/10.1016/j.jiec.2017.09.045